Work fluctuations in a time-dependent harmonic potential: Rigorous results beyond the overdamped limit

Chulan Kwon,[1] Jae Dong Noh,[2,3] and Hyunggyu Park[3]

[1]*Department of Physics, Myongji University, Yongin, Gyeonggi-Do 449-728, Korea*
[2]*Department of Physics, University of Seoul, Seoul 130-743, Republic of Korea*
[3]*School of Physics, Korea Institute for Advanced Study, Seoul 130-722, Korea*

We investigate the stochastic motion of a Brownian particle in the harmonic potential with a time-dependent force constant. It may describe the motion of a colloidal particle in an optical trap where the potential well is formed by a time-dependent field. We use the path integral formalism to solve the Langevin equation and the associated Fokker-Planck (Kramers) equation. Rigorous relations are derived to generate the probability density function for the time-dependent nonequilibrium work production beyond the overdamped limit. We find that the work distribution exhibits an exponential tail with a power-law prefactor, accompanied by an interesting oscillatory feature (multiple pseudo-locking-unlocking transitions) due to the inertial effect. Some exactly solvable cases are discussed in the overdamped limit.

I. INTRODUCTION

Nonequilibrium (NEQ) fluctuation has been an important issue in the field of statistical mechanics for the past two decades since the discovery of the fluctuation theorem for entropy production [1–3]. Fluctuation theorems (FTs) [4–11] and the Jarzynski equality (JE) [12,13] are the central theoretical relations governing NEQ fluctuation phenomena, widely valid for many NEQ systems, deterministic or stochastic, thermostated with heat baths. The NEQ fluctuation deals with a large fluctuation around the average with a considerable contribution from rare events. Such phenomena become dominant for a system with small degrees of freedom. There have been extensive studies of small experimental systems such as a microscopic bead dragging in a viscous fluid [14], a single molecule of RNA under mechanical stretch [15,16], an oscillating bead under the translating center of the optical trap [17], the circuit of an electric dipole in electric potential bias [18], and an ultralight metallic wire under torsion [19].

External bias was considered as a typical underlying mechanism for NEQ systems such as a nanocircuit device with potential bias [18,20], a harmonic oscillator under constant torque applied [19,21,22], and a one-dimensional lattice gas in contact at boundaries with different heat or particle baths [23,24]. A nonconservative force was also recognized as a source for the entropy production [6] such as in a nanoheat engine in contact with multiple reservoirs for a circulating current in high-dimensional systems [25–27]. The non-Markovian nature caused by a memory effect or colored noise is another source for NEQ [28,29]. In these examples, the system reaches a NEQ steady state (NESS) after a transient period, where a persistent nonzero current, directed or circulated, generates the incessant work production. The probability distribution function (PDF) of the work production exhibits an exponential decay with a power-law prefactor in the rare-event region [27], along with interesting unusual features such as an initial condition dependence of the large deviation function [30–33] and multiple dynamic transitions in reaching the NESS [27,34].

In contrast, a time-dependent perturbation on external parameters such as the electric field, magnetic field, volume, and force constant generates a genuine time-dependent NEQ state where the system never maintains the NESS. It is worth mentioning that there was an earlier work by Bochkov and Kuzovlev [35] in which the Hamiltonian dynamics with a perturbation linearly coupled to the time-dependent external force was studied and an equality similar to the JE was obtained. Its quantum mechanical version was also studied extensively [36–38]. The classical mechanical studies have concentrated on specific models. For example, the stochastic motion of a Brownian particle was studied in the harmonic potential moving with a constant velocity (the sliding parabola potential) [39–45] and also in the harmonic potential with a time-dependent force constant (the breathing parabola potential) [46–49]. In these cases, the work PDF also shows an exponential decay with a power-law prefactor in the rare-event region, along with a time-dependent characteristic value for the work production determining the exponential decay shape. Most of previous studies have considered the overdamped limit, partly because the experimental situation for a colloidal particle in a harmonic trap can be well approximated in the overdamped limit and also partly because the analytical treatment is much simpler [39–44,46–49].

In this paper we generalize these results beyond the overdamped limit (the underdamped case) for a Brownian particle in a breathing parabola potential with the momentum variable kept intact. We focus on the inertial effect on the time-dependent characteristic value for the work production. Our model may also serve as a soft-wall version of the box expansion or compression with a single Brownian particle inside, in contact with a thermal reservoir [50]. The experimental setup is also feasible: In a molecular tweezers or an optical trap experiment, the potential well can be approximated by the harmonic potential. The shape of the harmonic potential characterized by the force constant is set to vary with a time-dependent external field.

The importance of the underdamped dynamics has been overlooked so far except for a few cases [51]. Recent studies

have revealed crucial differences from the overdamped cases, such as in the fluctuation property of the housekeeping contribution to the total entropy production [52,53] and in the presence of the anomalous entropy production [54]. The theoretical formalism developed in this study will be useful for further studies in this direction in future.

The stochastic motion is described by the Langevin equation and the corresponding Fokker-Planck (Kramers) equation. We use the path integral formalism to derive rigorous relations from which the time-dependent work PDF and its cumulants can be easily calculated with machine accuracy. We find an interesting oscillatory feature of the work PDF shape, solely due to the inertial effect (absent in the overdamped limit). This resembles multiple locking-unlocking dynamic transitions found in the linear diffusion system [27,34], but shows smooth crossovers rather than sharp transitions. Thus we call this crossover as a pseudo-locking-unlocking transition. The key ingredient of dynamics evoking this interesting transition is the existence of the probability current under a periodic potential. In the underdamped case, the phase-space circulating current plays the role. Therefore, this phenomenon should be observed in more general multidimensional dynamic motions in NEQ systems. However, a full intuitive understanding calls for further investigation in the future.

In Sec. II we introduce the breathing harmonic potential function and discuss the FTs. In Sec. III we derive the equations for the PDF and the cumulants for the work production using the path integral formalism. Our formalism is tested for the systems in the sudden change limit. In Sec. IV we present the analysis for the work PDF and find the exponential tail with a power-law prefactor. In Sec. V we study the overdamped limit for exactly solvable cases. In Sec. VI we summarize the main results and discuss the perspective for future work.

II. TIME-DEPENDENT HARMONIC POTENTIAL

We consider the Brownian motion of a particle in one dimension under the breathing harmonic potential with a time-dependent force constant $k = k(t)$ and in contact with a heat bath. The equations of motion are given by

$$\dot{x} = p/m,$$
$$\dot{p} = -\gamma p/m - kx + \xi, \quad (1)$$

where γ is the damping coefficient and ξ is the white noise with zero mean satisfying $\langle \xi(t)\xi(t')\rangle = 2d\delta(t - t')$. The diffusion coefficient d is chosen to satisfy the Einstein relation $d = \beta^{-1}\gamma$, which guarantees the equilibrium (EQ) Boltzmann distribution at inverse temperature β in the steady state, if k is constant in time.

The equations of motion can be rewritten as

$$\dot{\mathbf{q}} = -\mathsf{F} \cdot \mathbf{q} + \boldsymbol{\zeta}, \quad (2)$$

where $\mathbf{q} \equiv (x,p)^T$ and $\boldsymbol{\zeta} \equiv (0,\xi)^T$. Here the superscript T denotes the transpose of a vector or a matrix. The force matrix F is given by

$$\mathsf{F} = \begin{pmatrix} 0 & -1/m \\ k & \gamma/m \end{pmatrix}. \quad (3)$$

The energy of a particle is given by $E(\mathbf{q};k) = \frac{p^2}{2m} + \frac{kx^2}{2}$, which is written as $E = \frac{1}{2}\mathbf{q}^T \cdot \mathsf{H} \cdot \mathbf{q}$ with a Hamiltonian matrix

$$\mathsf{H} = \begin{pmatrix} k & 0 \\ 0 & 1/m \end{pmatrix}. \quad (4)$$

Let $P(\mathbf{q},t)$ be the probability density function for finding a particle at state $\mathbf{q}$ and time t. Then it satisfies the Fokker-Planck equation

$$\frac{\partial P(\mathbf{q},t)}{\partial t} = \nabla \cdot (\mathsf{F} \cdot \mathbf{q} + \mathsf{D} \cdot \nabla) P(\mathbf{q},t), \quad (5)$$

where $\nabla = (\partial_x, \partial_p)^T$ and the diffusion matrix is given by

$$\mathsf{D} = \begin{pmatrix} \epsilon & 0 \\ 0 & d \end{pmatrix}, \quad (6)$$

where a small positive parameter ϵ is introduced to make it possible to invert the diffusion matrix D during a formal manipulation in the path integral formulation. In the end, we take the $\epsilon \to 0$ limit to recover the δ-function constraint $\delta(\dot{x} - p/m)$ for position and momentum; then the resultant equation becomes the Kramers equation.

With ϵ, position and momentum can be treated on the same footing, which gives us the formal advantage over the usual path integral with the δ-function constraint. This approach works well. For instance, one can reproduce the expected results for the EQ PDF when k is a time-independent constant [55]. In this case, the EQ Boltzmann distribution

$$P_{eq}(\mathbf{q};k) = \frac{1}{Z(k)} e^{-\beta E(\mathbf{q};k)} \quad (7)$$

becomes the stationary solution of the Kramers equation in the limit $\epsilon \to 0$. The partition function is given by $Z(k) = \int d\mathbf{q} e^{-\beta E(\mathbf{q};k)} = (4\pi^2 m/\beta^2 k)^{1/2}$, so the free energy is given by $\mathcal{F}(k) = -\frac{1}{2\beta} \ln(4\pi^2 m/\beta^2 k)$.

When the force constant k varies in time, the system is driven into a NEQ state. It belongs to the Jarzynski criterion for NEQ, where the rate of the work production is given by $\dot{\mathcal{W}} = \dot{k}(\partial E/\partial k)$. Then the NEQ work $\mathcal{W}$ done on the particle moving along a path $\mathbf{q}(\tau)$ for $0 < \tau < t$ is given by

$$\beta \mathcal{W}[\mathbf{q}] = \beta \int_0^t d\tau \dot{k} \frac{\partial E(\mathbf{q}(\tau); k(\tau))}{\partial k} = \frac{\beta}{2} \int_0^t d\tau \dot{k} x^2. \quad (8)$$

In the case of the sliding harmonic potential, the energy is given by $E = \frac{p^2}{2m} + \frac{k}{2}(x - y)^2$, where $y = vt$ with the sliding velocity v. So the work production rate $\dot{\mathcal{W}} = \dot{y}\partial E/\partial y$ is equal to $-kv(x - vt)$, which is linear in x. This linearity allows the exact calculation of the work PDF, which is simply Gaussian [39–45]. In contrast, the work production rate in our study, $\dot{\mathcal{W}} = \frac{1}{2}\dot{k}x^2$, is quadratic in x, which leads to a non-Gaussian work PDF. The closed-form expression for the work PDF is not available in this case, but we will show in the next section that it can be expressed formally via a kernel matrix satisfying an ordinary matrix differential equation. Furthermore, its solution can be obtained numerically with machine accuracy, which provides very accurate information on the tail part of the work PDF.

The work production is rewritten in a matrix form as

$$\beta\mathcal{W}[\mathbf{q}] = \frac{1}{2}\int_0^t d\tau \mathbf{q}^T \cdot \Lambda \cdot \mathbf{q}, \tag{9}$$

where

$$\Lambda = \beta\dot{\mathsf{H}} = \begin{pmatrix} \beta\dot{k} & 0 \\ 0 & 0 \end{pmatrix}. \tag{10}$$

The system is assumed to be initially in EQ at β with $k(0) = k_i$ and will reach a final state with $k(t) = k_f$, which is certainly far from EQ. In this situation, the JE states

$$\langle e^{-\beta\mathcal{W}[\mathbf{q}]}\rangle = e^{-\beta\Delta\mathcal{F}}, \tag{11}$$

where $\langle\cdots\rangle$ denotes the average over all possible paths $\mathbf{q}(\tau)$ and $\Delta\mathcal{F}$ is the free energy difference $\mathcal{F}(k_f) - \mathcal{F}(k_i)$ at β. The JE can be trivially derived from the Crooks relation [5]

$$P_F(W) = e^{\beta(W-\Delta\mathcal{F})}P_R(-W), \tag{12}$$

where $P_F(W) = \langle\delta(W - \mathcal{W}[\mathbf{q}])\rangle_F$ is the PDF for the work production W during the forward process with the change from k_i to k_f and vice versa $P_R(W)$ for the reverse process. The JE and the Crooks relation can be proved for a general form of energy and external perturbation for the Langevin dynamics if the system is initially in EQ at β [11]. However, the explicit expression for $P(W)$ is not generally known. There are not many stochastic models that can be solved analytically for the PDF of fluctuating quantities. The breathing harmonic potential with a time-dependent force constant not only is analytically tractable, but can also serve as an appropriate model for the potential well in an optical tweezers or trap.

III. PATH INTEGRAL FORMALISM WITH TIME-DEPENDENT FORCE

The Fokker-Planck equation for a multivariate system with a linear drift force, known as the high-dimensional Ornstein-Uhlenbeck process, is solvable, i.e., the time-dependent PDF $P(\mathbf{q},t)$ can be obtained analytically [56,57]. Nonequilibrium properties for this process were investigated in the context of the circulating NESS current [25] and the violation of the fluctuation-dissipation relation [58]. Recently we revisited this system in the context of the fluctuation theorems [27], when the (nonconservative) drift force does not vary in time. The path integral formalism developed in that study can be extended to the present problem with a time-dependent drift represented by the time-dependent force matrix $\mathsf{F}(t)$ in Eq. (3) with $k = k(t)$.

To describe the NEQ fluctuations, it is convenient to introduce a path integral during time period t as

$$I(\mathbf{q}_1, \lambda; \mathbf{l}(\tau)) = \int d\mathbf{q}_0 P_{eq}(\mathbf{q}_0; k(0))$$
$$\times \int D[\mathbf{q}]\exp\left(-\int_0^t d\tau L(\mathbf{q}, \dot{\mathbf{q}}) - \lambda\beta\mathcal{W}[\mathbf{q}]\right.$$
$$\left.+ \int_0^t d\tau \mathbf{l}^T \cdot \mathbf{q}\right). \tag{13}$$

The initial PDF for $\mathbf{q}_0$ is chosen to obey the EQ Boltzmann distribution $P_{eq}(\mathbf{q}_0; k(0))$ as in Eq. (7) and $\int D[\mathbf{q}](\cdots)$ denotes the integration over all possible paths connecting $\mathbf{q}(0) = \mathbf{q}_0$

and $\mathbf{q}(t) = \mathbf{q}_1$ for $0 < \tau < t$. The Lagrangian L is given as

$$L(\mathbf{q}, \dot{\mathbf{q}}; \mathsf{F}) = \frac{1}{4}(\dot{\mathbf{q}} + \mathsf{F} \cdot \mathbf{q})^T \cdot \mathsf{D}^{-1} \cdot (\dot{\mathbf{q}} + \mathsf{F} \cdot \mathbf{q}). \tag{14}$$

The source term $\int d\tau \mathbf{l}^T \cdot \mathbf{q}$ is introduced for later use. Note that the exponent of the integrand is at most quadratic in $\mathbf{q}$. Hence the path integration can be computed exactly by Gaussian integration.

The quantity I is useful in calculating physical quantities of interest. For example, the PDF $P(\mathbf{q},t)$ is given by [59]

$$P(\mathbf{q},t) = I(\mathbf{q}, \lambda = 0; \mathbf{l}(\tau) = \mathbf{0}). \tag{15}$$

The PDF for the NEQ work production can be also calculated from I. First, we define a dimensionless quantity for the work as $w = \beta W$ for simplicity and introduce its generating function

$$\mathcal{G}(\lambda) \equiv \langle e^{-\lambda\beta\mathcal{W}}\rangle = \int dw\, e^{-\lambda w}P(w), \tag{16}$$

which can be calculated as

$$\mathcal{G}(\lambda) = \int d\mathbf{q}\, I(\mathbf{q}, \lambda; \mathbf{l}(\tau) = \mathbf{0}). \tag{17}$$

Note that the JE $\mathcal{G}(1) = \exp[-\beta\Delta\mathcal{F}]$ can be proven explicitly in this path integral formalism as well as the generalized Crooks relation as $\mathcal{G}_F(\lambda)/\mathcal{G}_R(1-\lambda) = \exp[-\beta\Delta\mathcal{F}]$, where F (R) denotes the forward (reverse) process. The PDF for the dimensionless work w is then obtained by the inverse Fourier transformation as

$$P(w) = \int \frac{d\lambda}{2\pi}e^{i\lambda w}\mathcal{G}(i\lambda). \tag{18}$$

For an arbitrary functional $\mathcal{A}[\mathbf{q}(\tau)]$, one can also calculate its ensemble-average value from I. Defining the cumulant generating function as

$$\mathcal{Z}[\mathbf{l}(\tau)] = \int d\mathbf{q}\, I(\mathbf{q}, \lambda = 0; \mathbf{l}(\tau)), \tag{19}$$

one finds that

$$\langle\mathcal{A}[\mathbf{q}]\rangle = \mathcal{A}\left[\frac{\delta}{\delta\mathbf{l}(\tau)}\right]\mathcal{Z}[\mathbf{l}(\tau)]\bigg|_{\mathbf{l}\to\mathbf{0}}. \tag{20}$$

We will use this relation to calculate the cumulants of the work.

The path integral (13) can be evaluated by using the methods developed in our recent study [27]. Here we will present the results without showing detailed steps of the calculation.

A. Probability distribution function

The PDF $P(\mathbf{q},t)$ is given by

$$P(\mathbf{q},t) = |\det[2\pi\mathsf{A}^{-1}(t)]|^{-1/2}e^{-\mathbf{q}^T \cdot \mathsf{A}(t)\cdot\mathbf{q}/2}, \tag{21}$$

where the kernel $\mathsf{A}(t)$ is a symmetric matrix, satisfying the differential equation as

$$\frac{d\mathsf{A}^{-1}}{dt} = 2\mathsf{D} - [\mathsf{F}(t)\mathsf{A}^{-1} + \mathsf{A}^{-1}\mathsf{F}^T(t)]. \tag{22}$$

The formal solution is given by

$$\mathsf{A}^{-1}(t) = 2\int_0^t d\tau\mathsf{U}(t; t-\tau)\mathsf{D}\mathsf{U}^T(t; t-\tau)$$
$$+ \mathsf{U}(t; 0)\mathsf{A}^{-1}(0)\mathsf{U}^T(t; 0), \tag{23}$$

with the initial condition $\mathsf{A}(0) = \beta\mathsf{H}(0)$. Here the evolution operator U is given by

$$\mathsf{U}(t;t') = \left[\exp\left(-\int_{t'}^{t}d\tau\mathsf{F}(\tau)\right)\right]_{TO}, \qquad (24)$$

where the subscript denotes the time-ordered product, and satisfies the differential equation

$$\frac{\partial}{\partial t}\mathsf{U}(t;t') = -\mathsf{F}(t)\mathsf{U}(t;t'), \qquad (25)$$

with $\mathsf{U}(t';t') = \mathsf{I}$ (the identity matrix).

In the absence of noises ($\mathsf{D} = 0$), $\mathsf{U}(t;t')$ describes the deterministic evolution by $\mathbf{q}(t) = \mathsf{U}(t;t')\mathbf{q}(t')$. When the force matrix is constant in time so that $\mathsf{U}(t,t') = e^{-(t-t')\mathsf{F}}$, one can do the integral in Eq. (23) and find the explicit solution for $\mathsf{A}(t)$ [see Eq. [21] in [27]]. For a general time-dependent $\mathsf{F}(t)$, it is difficult to treat U analytically. However, Eqs. (23) and (25) can be solved precisely by numerical integrations.

B. Work distribution function

The generating function for the work distribution in Eq. (17) involves the integration of the quantity I with nonzero λ. The work $\mathcal{W}[\mathbf{q}]$ coupled to λ is also quadratic in $\mathbf{q}$ [see Eq. (9)], hence the integration can be performed in the same way as was done for the PDF. After some algebra, one can derive

$$\ln\mathcal{G}(\lambda) = -\frac{\lambda}{2}\int_{0}^{t}d\tau\,\mathrm{Tr}[\tilde{\mathsf{A}}^{-1}(\tau;\lambda)\Lambda(\tau)], \qquad (26)$$

where $\Lambda = \beta\dot{\mathsf{H}}$ in Eq. (10) and $\tilde{\mathsf{A}}(\tau;\lambda)$ is the modified kernel due to $-\lambda\beta\mathcal{W}$ in Eq. (13). It is found to satisfy the nonlinear differential equation

$$\frac{d\tilde{\mathsf{A}}^{-1}}{d\tau} = 2\mathsf{D} - (\mathsf{F}\tilde{\mathsf{A}}^{-1} + \tilde{\mathsf{A}}^{-1}\mathsf{F}^{T}) - \lambda\tilde{\mathsf{A}}^{-1}\Lambda\tilde{\mathsf{A}}^{-1}, \qquad (27)$$

where the initial condition is given by $\tilde{\mathsf{A}}(0;\lambda) = \beta\mathsf{H}(0)$.

This nonlinear differential equation can be solved easily for $\lambda = 0$ and 1. The solution is $\tilde{\mathsf{A}}(\tau;0) = \mathsf{A}(\tau)$ in Eq. (23), while $\tilde{\mathsf{A}}(\tau;1) = \beta\mathsf{H}(\tau)$. Interestingly, $\tilde{\mathsf{A}}(\tau;1)$ corresponds to the kernel for $P(\mathbf{q},\tau)$ in the quasistatic process. Inserting this into Eq. (26), we find

$$\ln\mathcal{G}(1) = -\frac{1}{2}\int_{0}^{t}d\tau\left(\frac{\dot{k}}{k}\right) = -\frac{1}{2}\ln\left[\frac{k(t)}{k(0)}\right] = -\beta\Delta\mathcal{F}, \qquad (28)$$

which verifies the JE.

It is more convenient to rewrite Eq. (27) in terms of $\tilde{\mathsf{A}}(\tau;\lambda)$ as

$$\frac{d\tilde{\mathsf{A}}}{d\tau} = \lambda\Lambda + (\tilde{\mathsf{A}}\mathsf{F} + \mathsf{F}^{T}\tilde{\mathsf{A}}) - 2\tilde{\mathsf{A}}\mathsf{D}\tilde{\mathsf{A}}, \qquad (29)$$

along with an equivalent and more effective expression for the generating function replacing Eq. (26) as

$$\ln\mathcal{G}(\lambda) = \int_{0}^{t}d\tau\,\mathrm{Tr}[\mathsf{F}(\tau) - \tilde{\mathsf{A}}(\tau;\lambda)\mathsf{D}] - \frac{1}{2}\ln\frac{\det\tilde{\mathsf{A}}(t;\lambda)}{\det\tilde{\mathsf{A}}(0;\lambda)}. \qquad (30)$$

A similar result has been found in the time-independent case [27]. Equations (29) and (30) are ingredients for a numerical study of the work production distribution $P(w)$, which cannot

be expressed analytically in a closed form. Nonetheless, these two equations can be solved numerically with machine accuracy, which provides very precise information on the tail behavior of $P(w)$ associated with rare events. It would be very difficult to get this information by usual numerical simulations of the Langevin equation due to huge sampling errors. In particular, the exponentially decaying tail of $P(w)$ is manifested by the divergence of $\mathcal{G}(\lambda)$, which turns out to be fully captured by the singularity in the logarithmic boundary term in Eq. (30). Thus we will focus on the behavior of $\det\tilde{\mathsf{A}}(t;\lambda)$ in the next section.

One can observe that Eq. (29) becomes independent of β if $\tilde{\mathsf{A}}$ is scaled by β. This proves that $\mathcal{G}(\lambda)$ as well as $P(w)$ is independent of β. Therefore, $P(W)$ is simply equal to $\beta P(w)$ with $w = \beta W$. In the weak-noise (large-β) limit [46,47], the tail behavior of $P(w)$ for large $|w|$ determines exactly and fully the work distribution $P(W)$, except for a narrow central region $|W| < \beta^{-1}$. We will return to this issue later.

C. Cumulants of work production

The cumulant generating function in Eq. (19) is found as

$$\mathcal{Z}[\mathbf{l}] = \exp\left(\frac{1}{2}\int d\tau\int d\tau'\mathbf{l}^{T}(\tau)\cdot\Gamma(\tau,\tau')\cdot\mathbf{l}(\tau')\right). \qquad (31)$$

This form is expected because the Lagrangian is quadratic in $\mathbf{q}$ and the source field $\mathbf{l}(\tau)$ is linearly coupled to $\mathbf{q}$. The kernel $\Gamma(\tau,\tau')$ is given as

$$\Gamma(\tau,\tau') = \begin{cases} \mathsf{U}(\tau,\tau')\mathsf{A}^{-1}(\tau'), & \tau \geqslant \tau' \\ \mathsf{A}^{-1}(\tau)\mathsf{U}^{T}(\tau',\tau), & \tau < \tau' \end{cases} \qquad (32)$$

and $\Gamma(\tau,\tau') = \Gamma^{T}(\tau',\tau)$.

Using Eqs. (20) and (31), one can express the average of any functional of path $\mathbf{q}(\tau)$ in terms of $\Gamma(\tau,\tau')$. For example, the first and the second cumulant of the work are given by

$$\langle\mathcal{W}\rangle = \frac{1}{2}\int_{0}^{t}d\tau\,\mathrm{Tr}[\dot{\mathsf{H}}(\tau)\Gamma(\tau,\tau)],$$

$$\langle\mathcal{W}^{2}\rangle_{c} = \frac{1}{2}\int_{0}^{t}d\tau\int_{0}^{t}d\tau'\mathrm{Tr}[\Gamma(\tau,\tau')\dot{\mathsf{H}}(\tau')\Gamma^{T}(\tau,\tau')\dot{\mathsf{H}}(\tau)],$$

where $\langle\mathcal{W}^{2}\rangle_{c} = \langle\mathcal{W}^{2}\rangle - \langle\mathcal{W}\rangle^{2}$. Note that $\dot{H}_{11} = \dot{k}$ and $\dot{H}_{ab} = 0$ otherwise. Then the expressions become simpler:

$$\langle\mathcal{W}\rangle = \frac{1}{2}\int_{0}^{t}d\tau\,\dot{k}A_{11}^{-1}(\tau), \qquad (33)$$

$$\langle\mathcal{W}^{2}\rangle_{c} = \frac{1}{2}\int_{0}^{t}d\tau\int_{0}^{t}d\tau'\dot{k}(\tau)\dot{k}(\tau')[\Gamma_{11}(\tau,\tau')]^{2}. \qquad (34)$$

One can also find higher-order cumulants in terms of $\Gamma(\tau,\tau')$, which are nonzero in all orders. This implies that the PDF $P(w)$ should have a non-Gaussian form. The PDF shape will be discussed further in the next session.

D. Sudden change limit

A sudden change is a rare case in which one can calculate the work PDF exactly, even in the underdamped case. Suppose that the particle is in EQ under the harmonic potential with the force constant k_{i} and the force constant is changed abruptly to k_{f} at time $t = 0$ [46,47]. If the particle is in a state $\mathbf{q} = (x,p)^{T}$

just before the change ($t = 0^-$), its state still remains the same right after the change ($t = 0^+$) as well as the PDF $P(\mathbf{q},t)$. The only change occurs in the potential energy, which results in the energy change $\Delta E = E(\mathbf{q},k_f) - E(\mathbf{q},k_i) = \frac{1}{2}(k_f - k_i)x^2$ for state $\mathbf{q}$. Then the work production $\mathcal{W}(\mathbf{q}) = \Delta E$.

As the initial distribution is given by the EQ Boltzmann distribution, the PDF $P(x) = \int dp P_{eq}(\mathbf{q};k_i) = \sqrt{\beta k_i/2\pi}e^{-\beta k_i x^2/2}$. Then the PDF $P(w)$ of the dimensionless work $w = \beta\mathcal{W}$ can be easily derived using $P(w)dw = 2P(x)|dx|$, which yields that

$$P(w) = \begin{cases} \theta(w)\sqrt{\frac{a}{\pi}}w^{-1/2}e^{-aw}, & a > 0 \\ \theta(-w)\sqrt{\frac{|a|}{\pi}}|w|^{-1/2}e^{|a|w}, & a < 0 \end{cases} \quad (35)$$

where $a = k_i/(k_f - k_i)$ and $\theta(w)$ is the Heaviside step function.

The generating function $\mathcal{G}$ can be easily calculated, using Eq. (16), as

$$\mathcal{G}(\lambda) = \left(\frac{\lambda k_f + (1-\lambda)k_i}{k_i}\right)^{-1/2}, \quad (36)$$

which diverges at $\lambda = k_i/(k_i - k_f) = -a$ as expected. The JE is also seen from $\mathcal{G}(1) = (k_f/k_i)^{-1/2}$.

Our analytic formalism in the preceding sections can also reproduce $\mathcal{G}(\lambda)$. The sudden change in the potential function can be studied by considering

$$k(\tau) = k_i\theta(-\tau) + k_f\theta(\tau), \quad \dot{k}(\tau) = (k_f - k_i)\delta(\tau). \quad (37)$$

Integrating Eq. (29) from $\tau = 0^-$ to $\tau = 0^+$, one gets

$$\tilde{A}(0^+;\lambda) = \tilde{A}(0^-;\lambda) + \lambda\beta(k_f - k_i)\begin{pmatrix} 1 & 0 \\ 0 & 0 \end{pmatrix}$$

$$= \beta\begin{pmatrix} (1-\lambda)k_i + \lambda k_f & 0 \\ 0 & 1/m \end{pmatrix}, \quad (38)$$

where $\tilde{A}(0^-;\lambda) = \beta H(0^-)$ is used. Then, from Eq. (30), one can easily reproduce the result in Eq. (36). The cumulants of the work can be also easily calculated as

$$\langle w \rangle = \frac{k_f - k_i}{2k_i}, \quad \langle w^2 \rangle_c = \frac{(k_f - k_i)^2}{2k_i^2}. \quad (39)$$

IV. ANALYSIS OF WORK DISTRIBUTION

The analytic formalism developed in this paper is useful in investigating the work distribution $P(w)$ numerically, in particular, its tail behavior, in contrast to direct numerical integration of the equations of motion where we always face a statistics problem, becoming serious in rare-event regions. In this section we first present numerical data from the latter method to check fluctuation relations and get some insights into the nature of the work production distribution. Then the tail behavior of $P(w)$ is carefully examined by the former method.

We set $m = \gamma = \beta = 1$ without loss of generality by the simple rescaling of t, x, and p. Then the only relevant parameter is the force constant k. We will consider a special case of $k(t) = k_i(1 + \alpha t)$ for convenience, where $\dot{k}$ is a time-independent constant.

First, we check the JE and the Crooks relation from the direct numerical integration of the time-discretized equations of motion. We adopt the notation $X_n = X(t = t_n)$ for a time-dependent quantity $X(t)$, where $t_n = n\Delta t$ ($n = 0,1,2,\ldots$) are discretized times in units of Δt. Then the equations of motion are solved from the difference equations

$$x_{n+1} = x_n + (\Delta t)p_n,$$
$$p_{n+1} = p_n - (\Delta t)(p_n + k_n x_n) + \sqrt{2(\Delta t)}\eta_n,$$

where η_n are independent Gaussian-distributed random variables with zero mean and unit variance. An initial configuration $\mathbf{q}_0 = (x_0,p_0)$ is drawn from the EQ distribution of Eq. (7). The dimensionless NEQ work production $w_n = \beta\mathcal{W}_n$ up to time t_n is evaluated from the recursion relation

$$w_{n+1} = w_n + \frac{k_i\alpha}{4}(x_{n+1}^2 + x_n^2)\Delta t, \quad (40)$$

with $w_0 = 0$. Repeating the simulations N_S times, one can measure the PDF $P(w)$ and the generating function $\mathcal{G}(\lambda)$ numerically. Note that the work production w is always positive for $\alpha > 0$ and negative for $\alpha < 0$, independent of noise realizations.

In simulations, we take $\Delta t = 10^{-3}$ and $N_S = 10^7$. The force constant $k(t)$ is taken to vary linearly from $k_i = 1$ to $k_f = 4$ and from $k_i = 4$ to $k_f = 1$, which will be referred to as the forward and the reverse process, respectively. Figure 1(a) shows $P_F(w)$ for the forward process until $t = 3$ with $\alpha = 1$ and $P_R(w)$ for the reverse process with $\alpha = -1/4$. We compare $P_F(w)$ and $e^{w-\beta\Delta\mathcal{F}}P_R(-w)$ with $\beta\Delta\mathcal{F} = \frac{1}{2}\ln\frac{k_f}{k_i} = \ln 2$. They seem to overlap each other well [except for the region with very small $P(w)$], which supports the validity of the Crooks relation in Eq. (12).

In order to examine the PDF in detail, we compute the generating function $\mathcal{G}(\lambda) = \langle e^{-\lambda w}\rangle$. These are plotted in Fig. 1(b). The JE states that $\mathcal{G}(\lambda = 1) = e^{-\beta\Delta\mathcal{F}}$, where $\beta\Delta\mathcal{F} = \ln 2$ for the forward process and $-\ln 2$ for the reverse process. Indeed, the numerical curves pass through the JE
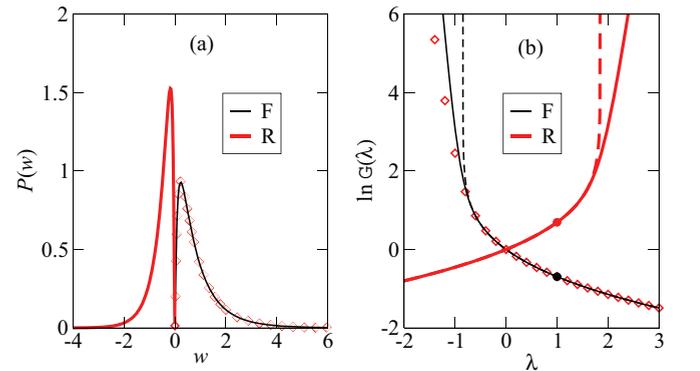
FIG. 1. (Color online) (a) Work distribution $P_F(w)$ for the forward (F) process (thin line) and $P_R(w)$ for the reverse (R) process (thick line). Open symbols represent $e^{w-\ln 2}P_R(-w)$. (b) Generating function $\mathcal{G}_F(\lambda)$ for the forward process and $\mathcal{G}_R(\lambda)$ for the reverse process. Closed symbols represent the JE points and open symbols represent $e^{-\ln 2}\mathcal{G}_R(1-\lambda)$. Also shown (dashed lines) are the generating functions obtained from the analytic formula in Eq. (30).
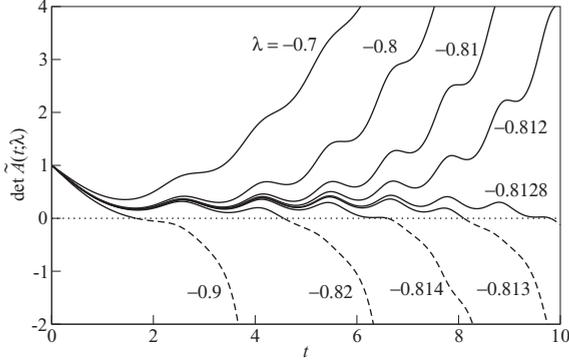
FIG. 2. Time evolution of $\det \tilde{A}(t; \lambda)$ for the case with $k(t) = k_i(1 + \alpha t)$, where $k_i = 1$ and $\alpha = 1$, at various values of λ.

points. We also compare $\mathcal{G}_F(\lambda)$ and $e^{-\beta \Delta \mathcal{F}} \mathcal{G}_R(1 - \lambda)$ to check the generalized Crooks relation. For moderate values of λ, both data align along a single curve. However, there is a slight discrepancy for large $|\lambda|$ where rare fluctuations with large values of $|w|$ are important. This reflects a statistical uncertainty due to limited samplings. Even with $N_S = 10^7$ samples, the statistics are poor for those rare fluctuations.

Now we utilize the analytic results in Eqs. (29) and (30), which are free from statistical errors, in order to determine the tail part of $P(w)$ precisely. In discretized times in the unit of $\Delta t = 10^{-3}$, the nonlinear differential equation (29) for $\tilde{A}(\tau; \lambda)$ is solved with the initial condition $\tilde{A}(0; \lambda) = \beta H(0)$ and the integration in Eq. (30) is performed numerically. We present the numerical results for the forward and reverse processes (dashed lines) in Fig. 1(b). As expected, the previous simulation results deviate significantly from our improved numerical results in rare-event regions. We checked that the relation $\mathcal{G}_F(\lambda) = e^{-\beta \Delta \mathcal{F}} \mathcal{G}_R(1 - \lambda)$ is satisfied perfectly well with our numerical results at all values of λ.

In fact, our numerical data in Fig. 1(b) show that $\mathcal{G}(\lambda)$ is divergent at thresholds λ_0 (forward) and $1 - \lambda_0$ (reverse) with $\lambda_0 \simeq -0.84713 < 0$. The divergence occurs when $\det \tilde{A}(t; \lambda) = 0$, as seen in Eq. (30). Figure 2 shows the time evolution of $\det \tilde{A}(t; \lambda)$ at several values of λ in the case with $k_i = 1$ and $\alpha = 1$. To a given value of t, $\det \tilde{A}$ becomes smaller as λ decreases and vanishes at a threshold λ_0. One can solve the equation $\det \tilde{A}(t; \lambda) = 0$ numerically to obtain the t-dependent threshold λ_0. Figure 3 shows the numerical results for the system with $k_i = 1$ and $\alpha = 0.5, 1$, and 2. The threshold depends on k_i and α and increases monotonically and converges to a finite limiting value $\lambda_0^\infty \simeq -1.39162, -0.81311$, and -0.48110 in the $t \to \infty$ limit.

The singular behavior of $\mathcal{G}(\lambda)$ reveals the asymptotic behavior of the tail shape of $P(w)$ for large $|w|$. Due to the generalized Crooks relation, it suffices to consider the forward process with positive α (compression). Figure 2 suggests that $\det \tilde{A}(t; \lambda)$ is regular near $\lambda = \lambda_0(t)$, so one can write $\det \tilde{A} \simeq c(\lambda - \lambda_0(t))$ with a positive constant c. Then, from Eq. (30), $\mathcal{G}(\lambda)$ diverges as

$$\mathcal{G}(\lambda) \sim [\lambda - \lambda_0(t)]^{-1/2}. \tag{41}$$
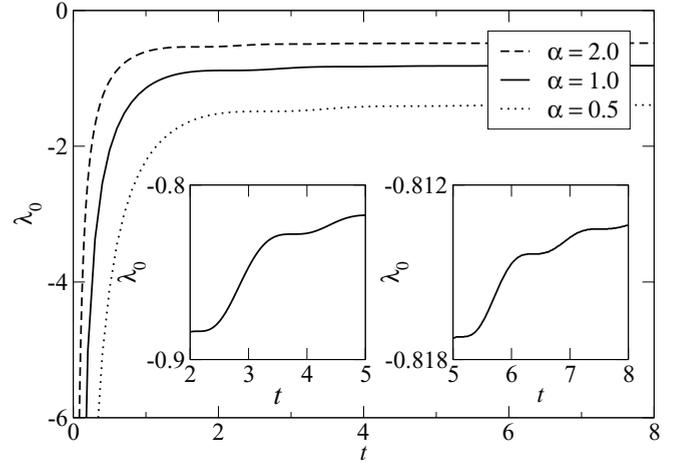
FIG. 3. The t dependence of the threshold λ_0 for the forward process with $k_i = 1$ and $\alpha = 0.5, 1, 2$. Multiple stepwise increases are observed in the insets showing the magnification of the curve with $\alpha = 1$.

The divergence at $\lambda = \lambda_0$ indicates that the work PDF has an exponential tail $P(w) \sim e^{-|\lambda_0|w}$ in the large-w region. This implies that the characteristic work cost for compressing a harmonic particle is given by $w_0 = 1/|\lambda_0|$. Furthermore, the inverse square-root singularity yields a power-law correction as [27]

$$P(w) \sim w^{-1/2} e^{-|\lambda_0(t)|w}. \tag{42}$$

Note that the abrupt change of k (sudden change limit) also yields the same tail, as was shown in the preceding section.

We test the tail shape by direct numerical integration of the equations of motion using $k_i = 1$, $k_f = 4$, and various $\alpha = 1, 2, 4, 8$. For each case, the threshold λ_0 is obtained by solving the equation $\det \tilde{A}(t; \lambda_0) = 0$ with fixed $t = (k_f - k_i)/k_i \alpha$. In Fig. 4 the PDF $P(w)$ multiplied by $e^{|\lambda_0|w}$ follows a power-law scaling for large w, which confirms the tail shape. Huge fluctuations for large w are due to statistical errors in sampling rare events.

The tail shape of $P(w)$ in Eq. (42) is consistent with previous findings in the overdamped limit [46–49]. It is also not
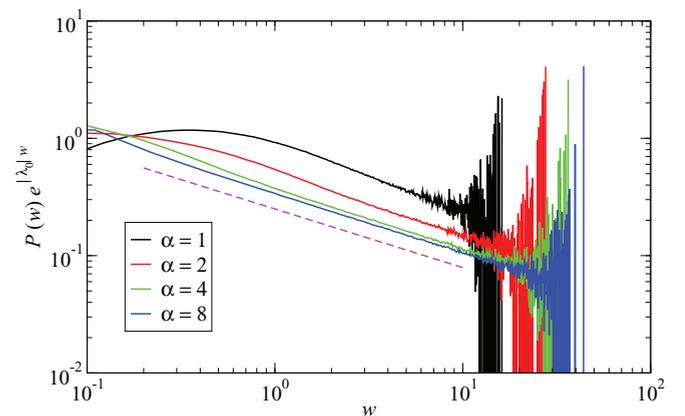
FIG. 4. (Color online) Rescaled PDF for the forward process with $k_i = 1$, $k_f = 4$, and $\alpha = 1, 2, 4, 8$ (from top to bottom). The dashed line has a slope of $-1/2$.

surprising to find that $|\lambda_0(t)|$ decreases with t because one can easily expect that the work PDF should be more distributed (flatter) as t increases. However, the monotonic behavior of $|\lambda_0(t)|$ is not trivially smooth, but has an interesting repeating structure in our underdamped case.

In Fig. 3 we observe a stepwise change of $|\lambda_0(t)|$ in time, composed of a rather fast linear change followed by quite slow plateau-type change, which repeats itself but with decreasing size in both magnitude and time period and finally converges to the limiting value of $|\lambda_0^\infty|$. This implies that the exponential tail of $P(w)$ relaxes into the limiting distribution via multiple (possibly infinitely many) fast-slow-type relaxation dynamics. These repeated fast-slow-type dynamics resemble multiple locking-unlocking dynamic transitions found in two-dimensional linear diffusion systems in the overdamped limit [34]. However, our case shows rather smooth crossovers between fast and slow dynamics, in contrast to sharp transitions with completely flat plateaus in $|\lambda_0(t)|$, reported in [34]. We call the stepwise changes in our case pseudo-locking-unlocking transitions. In mathematical language, we cannot find any $\det \tilde{\mathsf{A}}(t;\lambda)$ curve tangential to the t axis ($\det \tilde{\mathsf{A}} = 0$) in Fig. 2, which prohibits a completely flat plateau, so no sharp transition is realized.

It is easy to recognize that the oscillatory feature of $\det \tilde{\mathsf{A}}$ in Fig. 2 evokes the stepwise change of $|\lambda_0(t)|$. First, note that all $\det \tilde{\mathsf{A}}$ curves show oscillatory wiggles almost simultaneously in time and the oscillation frequency grows as t increases. So we can define a set of characteristic times $(t_1^\pm, t_2^\pm, \ldots)$ where all curves show a local minimum $(+)$ or maximum $(-)$ simultaneously, at least, approximately. The oscillatory behavior is related to the increasing frequency of the harmonic oscillator caused by the increasing force constant $k(t) = k_i(1 + \alpha t)$.

Due to this oscillatory feature of the $\det \tilde{\mathsf{A}}$ curves, one can easily figure out that the curves cross the t axis sparsely right after $t = t_1^+$ until $t = t_1^-$, densely for $t_1^- < t < t_2^+$, and so on. Therefore, λ_0 increases very fast during $0 < t < t_1^+$ and very slowly during $t_1^+ < t < t_1^-$ and this fast-slow relaxation dynamics repeats itself with increasing frequency.

The pseudo-locking-unlocking transitions are also manifested in physical observables such as the cumulants of the work production. Figure 5 shows the first cumulant $\langle w \rangle$ and second cumulant $\langle w^2 \rangle_c$ with $k_i = \alpha = 1$. These were evaluated
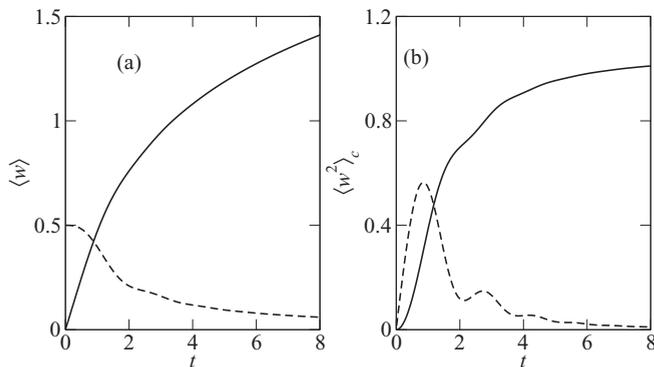
numerically using the expressions in Eqs. (33) and (34). The first cumulant $\langle w \rangle$ appears to be smoothly increasing in time, but one can observe its weak oscillatory behavior by looking at its time derivative. The second cumulant exhibits the clear stepwise increase. Note that the period of the steps coincides with that in λ_0 (see Fig. 3).

The underlying mechanism of these pseudo-locking-unlocking transitions should be similar to one for the sharp transitions found in the two-dimensional linear diffusion systems [34]. The only differences are the nature of the rotational current, which exists here only in the phase space of (x,p) and the time-dependent external force, which acts in the role of the rotational driving force as well as the (time-dependent) anisotropic harmonic potential in the phase space. However, we could not find a sharp dynamic transition in our model with an arbitrary choice of parameters (k_i, α). Recalling what we learned in [34], we guess that the anisotropy may be always small in our model, compared to the driving force magnitude, in order to avoid a sharp transition. This nontrivial behavior is characteristic of general multidimensional motions (including one-dimensional underdamped case), not specific to a certain type of protocol or potential shape. For a full understanding, however, further investigation is necessary.

For the overdamped one-dimensional case, we cannot have any rotational current, so the oscillatory behavior should be completely absent, which will be confirmed rigorously in the next section. Therefore, we conclude that the pseudo-locking-unlocking transitions found in the underdamped case originate from the existence of the rotational current in the phase space.

V. OVERDAMPED LIMIT

In the overdamped limit, the usual Fokker-Planck equation, replacing the Kramers equation, reads

$$\frac{\partial P(x,t)}{\partial t} = \frac{\partial}{\partial x}\left(\gamma^{-1}k(t)x + (\gamma\beta)^{-1}\frac{\partial}{\partial x}\right)P(x,t). \quad (43)$$

Our formalism developed in preceding sections can be applied also by replacing D with $(\gamma\beta)^{-1}$, F with $\gamma^{-1}k$, H with k, and $\dot{\mathsf{H}}$ with $\dot{k}$. Then the work generating function $\mathcal{G}(\lambda)$ is given by

$$\ln \mathcal{G}(\lambda) = \int_0^t d\tau \left(\frac{k(\tau)}{\gamma} - \frac{\tilde{A}(\tau;\lambda)}{\gamma\beta}\right) - \frac{1}{2}\ln\frac{\tilde{A}(t;\lambda)}{\tilde{A}(0;\lambda)}, \quad (44)$$

where the scalar quantity $\tilde{A}(t;\lambda)$ satisfies a nonlinear differential equation

$$\frac{d\tilde{A}(\tau;\lambda)}{d\tau} = (\beta\dot{k})\lambda + 2\frac{k}{\gamma}\tilde{A} - \frac{2}{\gamma\beta}\tilde{A}^2 \quad (45)$$

with the initial condition $\tilde{A}(0;\lambda) = \beta k(0) = \beta k_i$. We will set $\gamma = \beta = 1$ without loss of generality and consider two different choices of $k(\tau)$.

A. $k(\tau) = k_i(1 + \alpha\tau)$

All relevant information can be obtained from Eqs. (44) and (45). Unfortunately, the closed-form solution for $\tilde{A}(t;\lambda)$ or $\mathcal{G}(\lambda)$ is not available. However, the highly accurate numerical solution is possible, which is shown in Fig. 6(a) for $\tilde{A}(t;\lambda)$ with $k_i = 1$ and $\alpha = 1$. As in the Brownian dynamics, it becomes zero at a t-dependent threshold λ_0. The threshold is plotted

FIG. 5. (a) First cumulant and (b) second cumulant. Solid lines are for the cumulants, while the dashed lines are for their time derivatives.
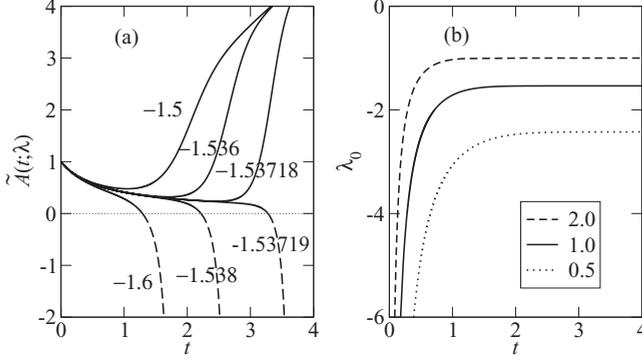
FIG. 6. (a) Time evolution of $\tilde{A}(t;\lambda)$ in the overdamped case with $k_i = 1$ and $\alpha = 1$ at various values of λ. (b) The t dependence of the threshold λ_0 for the processes with $k_i = 1$ and $\alpha = 0.5, 1, 2$.

in Fig. 6(b). From the similar analysis for Eq. (41), the PDF $P(w)$ can be found to have the same tail shape as in Eq. (42). Note that the particle dynamics does not display any oscillatory motion in the overdamped limit, hence $\tilde{A}$ does not either, as shown in Fig. 6(a). Thus the threshold λ_0 in Fig. 6(b) varies in time smoothly, showing no stepwise change at all.

Engel and Nickelsen studied the same harmonic potential problem in the overdamped limit [46,47]. In their studies they evaluated the path integral using the saddle point method in the low-noise (large-β) limit. However, as pointed out in Sec. III, $P(w)$ is independent of β, so $P(W)$ with $w = \beta W$ can be *exactly* determined from the tail behavior of $P(w)$ except for $|W| < \beta^{-1}$.

In order to calculate the cumulants of the work production, we need to evaluate the PDF kernel $A(t)$, first, using Eqs. (23) and (24). As we do not need to deal with the time-ordered product, we simply gets $U(t,t') = \exp[-\int_{t'}^{t} d\tau k(\tau)]$. Then one can explicitly calculate the cumulants for the work production. Using Eqs. (23) and (32) we find

$$A^{-1}(t) = 2 \int_0^t d\tau \exp\left(-2 \int_\tau^t d\tau' k(\tau')\right)$$
$$+ k_i^{-1} \exp\left(-2 \int_0^t d\tau k(\tau)\right) \qquad (46)$$

and

$$\Gamma(t,t') = \exp\left(-\int_{t'}^{t} d\tau k(\tau)\right) A^{-1}(t'), \qquad (47)$$

where we use $A^{-1}(0) = k_i^{-1}$.

For $k(\tau) = k_i(1 + \alpha\tau)$ we find

$$A^{-1}(t) = k_i^{-1} e^{-2k_i t - k_i \alpha t^2} g(t) \qquad (48)$$

and

$$\Gamma(t,t') = k_i^{-1} e^{-k_i(t+t') - k_i \alpha(t^2+t'^2)/2} g(t'), \qquad (49)$$

where

$$g(t) = 1 + 2k_i \int_0^t d\tau e^{2k_i \tau + k_i \alpha \tau^2}. \qquad (50)$$

The first and second cumulants are found as

$$\langle w \rangle = \frac{\alpha}{2} \int_0^t d\tau e^{-2k_i \tau - k_i \alpha \tau^2} g(\tau), \qquad (51)$$

$$\langle w^2 \rangle_c = \frac{\alpha^2}{2} \int_0^t d\tau \left\{ \int_0^\tau d\tau' h(\tau,\tau') g(\tau')^2 \right.$$
$$\left. + \int_\tau^t d\tau' h(\tau,\tau') g(\tau)^2 \right\}, \qquad (52)$$

where

$$h(\tau,\tau') = e^{-2k_i(\tau+\tau') - k_i \alpha(\tau^2+\tau'^2)}. \qquad (53)$$

There are two extreme cases: quasistatic and sudden processes. For the quasistatic process, one can take the limits $\alpha \to 0$ and $t \to \infty$ with a finite value of $\alpha t = (k_f - k_i)/k_i$. Changing the variable as $u = k_i \alpha \tau / (k_f - k_i)$, one can get the approximate result for the time integral. The important ingredient for the integration is

$$\int_a^b du e^{cu^2} \to \frac{1}{2c} \left(\frac{e^{cb^2}}{b} - \frac{e^{ca^2}}{a} \right),$$

where $c = (k_f - k_i)^2 / k_i \alpha \to \infty$. The final results are

$$\langle w \rangle = \frac{1}{2} \ln\left(\frac{k_f}{k_i}\right) + \frac{\alpha}{8} \frac{k_f^2 - k_i^2}{k_i k_f^2} + O(\alpha^2),$$
$$\langle w^2 \rangle_c = \frac{\alpha}{4} \frac{k_f^2 - k_i^2}{k_i k_f^2} + O(\alpha^2), \qquad (54)$$

which agree with the results by Speck [48]. This indicates that the work distribution function is perfectly Gaussian centered around $w = \beta \Delta\mathcal{F}$ up to $O(\alpha)$ and the non-Gaussianity starts to appear in $O(\alpha^2)$ [60]. In the quasistatic limit ($\alpha \to 0$), the work distribution function becomes a δ function, as expected for the EQ processes.

For a sudden process, one can take the opposite limits $\alpha \to \infty$ and $t \to 0$ with a finite value of $\alpha t = (k_f - k_i)/k_i$. Also using the same variable u, the integrand of $\int_a^b du e^{cu^2}$ can be expanded in orders of c in the $c \to 0$ limit. As a result, we find

$$\langle w \rangle = \frac{k_f - k_i}{2k_i} \left(1 - \frac{(k_f - k_i)^2}{3k_i \alpha}\right) + O(\alpha^{-2}),$$
$$\langle w^2 \rangle_c = \frac{(k_f - k_i)^2}{2k_i^2} \left(1 - \frac{2(k_f - k_i)}{3\alpha}\right) + O(\alpha^{-2}). \qquad (55)$$

Note that $\langle w \rangle$ and $\langle w^2 \rangle_c$ are finite even for an instantaneous change ($\alpha = \infty$), which agrees with the sudden change limit for the underdamped case in Eq. (39). It is different from the case for the rigid wall moving with speed v in the $v \to \infty$ limit, where we expect $\langle w \rangle \to 0$ [50]. The difference is due to the distinctive situations. For the former, the collision occurs everywhere with the harmonic potential, while for the latter the collision occurs only at the descending wall. The similarity lies in the nontrivial fluctuation around the average value.

B. $k(\tau) = k_i/(1 + \alpha\tau)$

With this specific form, one can find the closed-form solution for the work generating function $\mathcal{G}(\lambda)$. For $\alpha > 0$, the harmonic potential becomes flatter with time $\tau \geqslant 0$ and the work w done on the particle is always negative. In contrast, for $\alpha < 0$, the harmonic potential becomes stiffer with time τ ($0 \leqslant \tau < 1/|\alpha|$) and w is always positive.

It is convenient to change the variables as

$$f_\lambda(u) \equiv (1 + \alpha\tau)\tilde{A}(\tau; \lambda), \tag{56}$$

$$u \equiv \frac{1}{\alpha}\ln(1 + \alpha\tau). \tag{57}$$

The timelike variable u is monotonically increasing with τ, starting from 0 to ∞ for any nonzero α. From Eq. (45) one obtains a differential equation for $f_\lambda(u)$:

$$\frac{df_\lambda}{du} = -2[(f_\lambda - c)^2 + \kappa^2], \tag{58}$$

with $\kappa = \sqrt{\tilde{\lambda} - c^2}$, $c = (2k_i + \alpha)/4$, and $\tilde{\lambda} = \alpha k_i \lambda/2$. Note that κ may be either positive real or pure imaginary, depending on the range of $\tilde{\lambda}$. In either case, the solution is given by

$$f_\lambda(u) = \frac{k_i\cos(2\kappa u) + (ck_i - \tilde{\lambda})\frac{\sin(2\kappa u)}{\kappa}}{\cos(2\kappa u) + (k_i - c)\frac{\sin(2\kappa u)}{\kappa}}, \tag{59}$$

with $\cos(ix) = \cosh x$ and $\sin(ix) = i\sinh x$ for any x.

With the solution for $f_\lambda(u)$ or, equivalently, for $\tilde{A}(\tau; \lambda)$, one can obtain the work generating function using Eq. (44). It is useful to note that $f_\lambda(u) = c + \frac{1}{2}\frac{d}{du}\ln[\cos(2\kappa u) + (k_i - c)\sin(2\kappa u)/\kappa]$. After straightforward algebra, we find that

$$\mathcal{G}(\lambda) = \frac{e^{cu_t}}{\sqrt{\cos(2\kappa u_t) + \frac{ck_i - \tilde{\lambda}}{k_i}\frac{\sin(2\kappa u_t)}{\kappa}}}, \tag{60}$$

with $u_t = \frac{1}{\alpha}\ln(1 + \alpha t)$.

The work PDF $P(w)$ can be obtained by the inverse Fourier transformation of $\mathcal{G}(\lambda)$ in Eq. (18). First, note that the generating function has the inverse square-root singularity at a particular value of $\lambda = \lambda_0(u)$ where the denominator in Eq. (60) vanishes. As discussed before, this leads to

$$P(w) \sim \frac{1}{|w|^{1/2}}e^{\lambda_0(u)w} \tag{61}$$

in the $\omega \to -\infty$ limit for $\alpha > 0$ ($\lambda_0 > 0$) or in the $\omega \to \infty$ limit for $\alpha < 0$ ($\lambda_0 < 0$).

In fact, the singularity occurs when $\tilde{A}(\tau; \lambda) = 0$ or, equivalently, $f_\lambda(u) = 0$, which yields the relation for the singular point as

$$u_t = \frac{1}{2\sqrt{\tilde{\lambda}_0 - c^2}}\tan^{-1}\left(\frac{k_i\sqrt{\tilde{\lambda}_0 - c^2}}{\tilde{\lambda}_0 - ck_i}\right), \tag{62}$$

with $\tilde{\lambda}_0 = \alpha k_i \lambda_0/2$. It should be understood that $\tan^{-1}(ix) = i\tanh^{-1}(x)$ and that $0 \leqslant \tan^{-1}x < \pi$ for a real x. Figure 7 shows the plots for the solution of Eq. (62), where the divergence of u_t is observed as $\tilde{\lambda}_0$ approaches the limiting value from above. Interestingly, the time dependence and the limiting value are very different, depending on whether $c < 0$ ($\alpha \leqslant -2k_i$), $0 \leqslant c < k_i$ ($-2k_i < \alpha \leqslant 2k_i$), or $k_i \geqslant c$ ($\alpha > 2k_i$). In particular, the limiting value $\lambda_0^\infty = \lim_{u\to\infty}\lambda_0$ is given by

$$\lambda_0^\infty = \begin{cases} 0 & (\alpha \leqslant -2k_i) \\ \frac{(2k_i + \alpha)^2}{8k_i\alpha} & (-2k_i < \alpha \leqslant 2k_i) \\ 1 & (\alpha > 2k_i). \end{cases} \tag{63}$$

We present the plot of λ_0^∞ as a function of α/k_i in Fig. 8.
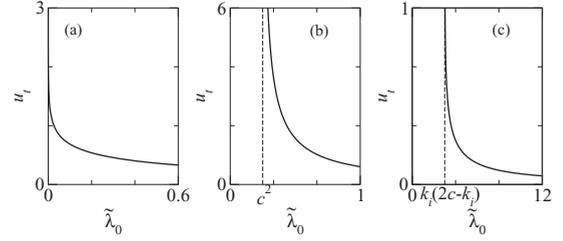
FIG. 7. Curves representing the relation between $u_t = \frac{1}{\alpha}\ln(1 + \alpha t)$ and $\tilde{\lambda}_0 = \alpha k_i \lambda_0/2$ for (a) $c < 0$, (b) $0 < c < k_i$, and (c) $k_i < c$. The values of (c, k_i) are taken to be $(-1, 1)$, $(1/2, 1)$, and $(2, 1)$, respectively.

There is an interesting symmetry of $\lambda_0^\infty(-\alpha) = 1 - \lambda_0^\infty(\alpha)$. This comes from the Crooks relation. The reverse protocol with respect to the forward protocol $k(\tau) = k_i/(1 + \alpha\tau)$ should be given as $k_r(\tau) = k(t - \tau) = k_f/(1 + \alpha_r\tau)$, with $\alpha_r = -\alpha k_f/k_i$ and $k_f = k_i/(1 + \alpha t)$. If the system starts with the EQ distribution with $k_r(0) = k_f$, all results derived here can be applied also for the reverse process by replacing k_i by k_f and α by $-\alpha k_f/k_i$. Then Eq. (63) gives us $\lambda_{0,r}^\infty(\alpha_r) = \lambda_0^\infty(-\alpha)$. The Crooks relation of Eq. (12) yields $\lambda_0^\infty = 1 - \lambda_{0,r}^\infty$ in the large-w limit, which leads to our symmetry of $\lambda_0^\infty(-\alpha) = 1 - \lambda_0^\infty(\alpha)$.

We add a few remarks on the interesting α dependence of λ_0^∞.

(i) For $\alpha \geqslant 2k_i$, the tail shape of $P(w)$ does not change with α and $\lambda_0^\infty = 1$. When α is large enough, the harmonic potential flattens very fast. Then the particle dynamics starting from the EQ distribution with k_i would be rather localized and not fully relaxed into the flattened harmonic potential. So the fluctuation in w may be dominated by an initial transient behavior even in the long-time limit ($t \to \infty$), independent of the detailed shape of $k(t)$. The sudden change limit discussed in Sec. III D corresponds to the $\alpha = \infty$ limit with $k_f = 0$, where $\lambda_0^\infty = |k_i/(k_f - k_i)| = 1$ from Eq. (35) is consistent with the result for $\alpha \geqslant 2k_i$. Nevertheless, it is still quite remarkable to find $\lambda_0^\infty = 1$ for large but finite α. Similar features of the initial-distribution dominance in the large
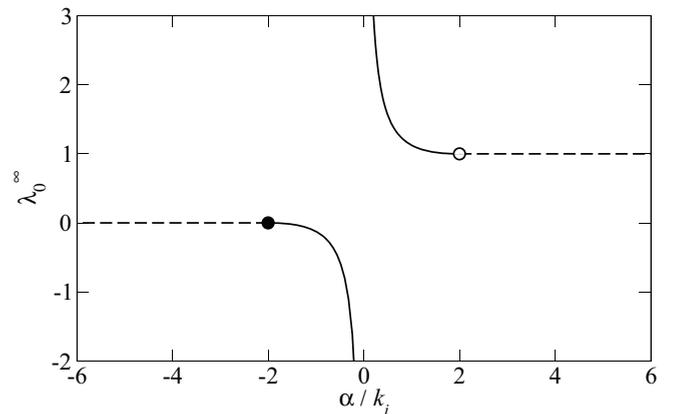
FIG. 8. Plot of λ_0^∞ versus α/k_i. The dashed lines are a flat straight line of $\lambda_0^\infty = 1$ starting from the $\alpha/k_i = 2$ point (open circle) and of $\lambda_0^\infty = 0$ starting from the $\alpha/k_i = -2$ point (closed circle).

deviation function in the long-time limit have been found in various different situations [30–33].

(ii) For $|\alpha| < 2k_i$, $|\lambda_\infty|$ decreases monotonically as $|\alpha|$ increases. This behavior is compatible with the common wisdom that the fluctuation gets stronger [longer tail in $P(\omega)$] as the rate of the change in driving increases.

(iii) When $\alpha \leqslant -2k_i$ (or $c \leqslant 0$) we obtain $\lambda_0^\infty = 0$. This implies that $P(\omega)$ has a pure power-law tail in the positive-w region in the $u \to \infty$ ($t \to 1/|\alpha|$) limit. In this case, the driving is strong enough to generate huge power-law-type fluctuations.

The transient behavior of λ_0 is also investigated in two limits. In the short-time limit ($u_t \to 0$), $P(w)$ is expected to exhibit a δ-function distribution centered at $w = 0$. This is confirmed by the solution of Eq. (62): $\tilde{\lambda}_0 \simeq k_i/(2u_t)$ or $\lambda_0 \simeq 1/(\alpha u_t)$ in the $u_t \to 0$ limit. In the opposite limit ($u_t \to \infty$), Eq. (62) yields

$$
\tilde{\lambda}_0 \simeq
\begin{cases}
\dfrac{4c^2 k_i}{k_i - 2c} e^{4cu_t} & (c < 0) \\[2mm]
\dfrac{\pi^2}{16u_t^2} & (c = 0) \\[2mm]
c^2 + \dfrac{\pi^2}{4u_t^2} & (0 < c < k_i) \\[2mm]
c^2 + \dfrac{\pi^2}{16u_t^2} & (c = k_i) \\[2mm]
k_i(2c - k_i) + \dfrac{4k_i(c - k_i)^2}{2c - k_i} e^{-4(c - k_i)u_t} & (c > k_i).
\end{cases}
\tag{64}
$$

Note that the asymptotic behavior near $\tilde{\lambda} = \tilde{\lambda}_0^+$ is very different, depending on the region. In terms of λ_0 and t, it is interesting to see a nontrivial power-law relaxation for $\alpha > 2k_i$ ($k_i < c$) such that $\lambda_0 \simeq 1 + z^2(1 + \alpha t)^{-z}$ with $z = 1 - 2k_i/\alpha$.

The generating function also produces the cumulants of the work production by $\langle w^n \rangle_c = d^n \ln \mathcal{G}/d(-\lambda)^n|_{\lambda=0}$. We focus on the mean value of the work, which is given by

$$
\langle w \rangle = -\frac{\alpha}{4c}\left[k_i u_t + \frac{1}{2}\left(1 - \frac{k_i}{2c}\right)(1 - e^{-4cu_t}) \right].
\tag{65}
$$

The quasi-static process corresponds to the limiting case where $\alpha \to 0$, $t \to \infty$ with fixed $\alpha t = (k_i - k_f)/k_f$. In this limit, we find

$$
\langle w \rangle = -\frac{1}{2}\ln(1 + \alpha t) = \frac{1}{2}\ln\left(\frac{k_f}{k_i}\right)
\tag{66}
$$

which agrees with Eq. (54). For a sudden process, we take the opposite limit where $\alpha \to \infty$, $t \to 0$ with the same fixed value of αt in the above. Eq. (65) approaches $\langle w \rangle = (k_f - k_i)/2k_i$, which agrees with Eq. (55).

VI. SUMMARY

The Brownian dynamics with both position x and momentum p variables has not been investigated in the context of the work production with a time-dependent protocol. In most literatures, the overdamped limit was taken for simplicity or due to many experiments with the overdamped time scale. Otherwise, the Kramers equation should be considered and investigated for the underdamped case, which is usually a nontrivial task.

We convert the Kramers equation into the usual Fokker-Planck equation by relaxing the strict constraint of $\delta(\dot{x} - p/m)$, where x and p can be put on the same footing

with the singular diffusion matrix introduced in Eq. (6). Then, the standard path-integral formalism can be applied also to the underdamped case. This approach is well-known even at the textbook level, but there are not many examples exploiting this method. In our study, we have shown that this approach is very useful in finding the results analytically and also numerically, by examining the work fluctuations of a Brownian particle in the breathing harmonic potential beyond the overdamped limit. It should be straightforward to apply our formalism to a more complex time-dependent harmonic potential such as a combination of the sliding and breathing potentials.

In the case of the breathing harmonic potential with a time-dependent force constant $k(t)$, we derived the generating function for the work production rigorously via the first-order ordinary matrix differential equation, which can be solved numerically with machine accuracy. As a result, we found the exponential tail with a power-law prefactor in the PDF $P(w)$ and the characteristic work production $1/|\lambda_0(t)|$, which increases with time t. Remarkably, the time-dependence of $|\lambda_0(t)|$ exhibits an interesting fine structure of the infinite but not sharply-edged staircase. By comparing the multiple locking-unlocking transitions (sharply-edged staircase) found in the two-dimensional linear diffusion system [34], we call these rather smooth staircase as a manifestation of multiple pseudo locking-unlocking transitions. These pseudo transitions completely go away in the overdamped limit where no rotational current exists even in the phase space. We expect that these interesting transitions should be present in most of multi-dimensional dynamics in NEQ systems. We also consider some exactly solvable models in the overdamped limit and found an interesting power-law (not exponential) tail in $P(w)$ for the case of rather fast compression ($\alpha \leqslant -2k_i$) with the protocol $k(t) = k_i/(1 + \alpha t)$, which implies huge NEQ fluctuations.

The potential well in optical tweezers or an optical trap experiment is controlled by an external field, so one can make a continuous shape change in time by applying a time-varying external field. Therefore, our study can serve as a theoretical basis for such experiments, since the potential well may be approximated to be harmonic in many cases. The perturbation theory might be developed to investigate an anharmonic effect. Our recent study of the multi-dimensional diffusion dynamics for a linear drift force [27,34] in the overdamped limit can be also realized in such experiments. It would be very interesting to observe the (pseudo) locking-unlocking dynamic transitions in experiments by measuring the work PDF or its cumulants.

[1] D. J. Evans, E. G. D. Cohen, and G. P. Morriss, Phys. Rev. Lett. **71**, 2401 (1993).

[2] D. J. Evans and D. J. Searles, Phys. Rev. E **50**, 1645 (1994); **52**, 5839 (1995); **53**, 5808 (1996).

[3] G. Gallavotti and E. G. D. Cohen, Phys. Rev. Lett. **74**, 2694 (1995); J. Stat. Phys. **80**, 931 (1995).

[4] G. Gallavotti, Phys. Rev. Lett. **77**, 4334 (1996).

[5] G. E. Crooks, J. Stat. Phys. **90**, 1481 (1998).

[6] J. Kurchan, J. Phys. A: Math. Gen. **31**, 3719 (1998).

[7] J. L. Lebowitz and H. Spohn, J. Stat. Phys. **95**, 333 (1999).

[8] C. Maes, J. Stat. Phys. **95**, 367 (1998).

[9] T. Hatano and S. I. Sasa, Phys. Rev. Lett. **86**, 3463 (2001).

[10] U. Seifert, Phys. Rev. Lett. **95**, 040602 (2005).

[11] J. Kurchan, J. Stat. Mech. (2007) P07005.

[12] C. Jarzynski, Phys. Rev. Lett. **78**, 2690 (1997); Phys. Rev. E **56**, 5018 (1997); J. Stat. Phys. **98**, 77 (2000).

[13] G. E. Crooks, Phys. Rev. E **61**, 2361 (2000).

[14] G. M. Wang, E. M. Sevick, E. Mittag, D. J. Searles, and D. J. Evans, Phys. Rev. Lett. **89**, 050601 (2002).

[15] G. Hummer and A. Szabo, Proc. Natl. Acad. Sci. **98**, 3658 (2001).

[16] J. Liphard, S. Dumont, S. B. Smith, I. Tinico, Jr., and C. Bustamante, Science **296**, 1832 (2002).

[17] E. H. Trepagnier, C. Jarzynski, F. Ritort, G. E. Crooks, C. J. Bustamante, and J. Liphardt, Proc. Natl. Acad. Sci. **101**, 15038 (2004).

[18] N. Garnier and S. Ciliberto, Phys. Rev. E **71**, 060101 (2005).

[19] F. Douarche, S. Joubaud, N. B. Garnier, A. Petrosyan, and S. Ciliberto, Phys. Rev. Lett. **97**, 140603 (2006).

[20] S. Joubaud, N. B. Garnier, and S. Ciliberto, Europhys. Lett. **82**, 30007 (2008).

[21] F. Douarche, S. Ciliberto, and A. Petrosyan, J. Stat. Mech. (2005) P09011.

[22] S. Joubaud, N. B. Garnier, and S. Ciliberto, J. Stat. Mech. (2007) P09018; S. Joubaud, N. B. Garnier, F. Douarche, A. Petrosyan, and S. Ciliberto, C. R. Phys. **8**, 518 (2007).

[23] T. Bodineau and B. Derrida, C. R. Phys. **8**, 540 (2005).

[24] B. Derrida, J. Stat. Mech. (2007) P07023.

[25] C. Kwon, P. Ao, and D. Thouless, Proc. Nat. Acad. Sci. **102**, 13029 (2005).

[26] R. Filliger and P. Reimann, Phys. Rev. Lett. **99**, 230602 (2007).

[27] C. Kwon, J. D. Noh, and H. Park, Phys. Rev. E **83**, 061145 (2011).

[28] T. Speck and U. Seifert, J. Stat. Mech. (2007) L09002.

[29] A. Puglisi and D. Villamaina, Europhys. Lett. **88**, 30004 (2009).

[30] J. Farago, J. Stat. Phys. **107**, 781 (2002).

[31] P. Visco, J. Stat. Mech. (2006) P06006.

[32] A. Puglisi, L. Rondoni, and A. Vulpiani, J. Stat. Mech. (2006) P08010.

[33] J. S. Lee, C. Kwon, and H. Park, Phys. Rev. E **87**, 020104(R) (2013).

[34] J. D. Noh, C. Kwon, and H. Park, Phys. Rev. Lett. **111**, 130601 (2013).

[35] G. N. Bochkov and Yu. E. Kuzovlev, Sov. Phys. JETP **45**, 125 (1977).

[36] P. Talkner, E. Lutz, and P. Hänggi, Phys. Rev. E **75**, 050102(R) (2007); M. Campisi, P. Talkner, and P. Hänggi, Phys. Rev. Lett. **102**, 210401 (2009).

[37] C. M. Van Vliet, *Equilibrium and Non-equilibrium Statistical Mechanics*, Chapter XVIII (World Scientific, Singapore, 2010).

[38] C. M. Van Vliet, Phys. Rev. E **86**, 051106 (2012).

[39] O. Mazonka and C. Jarzynski, arXiv:cond-mat/9912121.

[40] R. van Zon and E. G. D. Cohen, Phys. Rev. Lett. **91**, 110601 (2003).

[41] R. van Zon and E. G. D. Cohen, Phys. Rev. E **67**, 046102 (2003).

[42] R. van Zon and E. G. D. Cohen, Phys. Rev. E **69**, 056121 (2004).

[43] T. Taniguchi and E. G. D. Cohen, J. Stat. Phys. **126**, 1 (2007).

[44] E. G. D. Cohen, J. Stat. Mech. (2008) P07014.

[45] A. Imparato, L. Peliti, G. Pesce, G. Rusciano, and A. Sasso, Phys. Rev. E **76**, 050101(R) (2007).

[46] A. Engel, Phys. Rev. E **80**, 021120 (2009).

[47] D. Nickelsen and A. Engel, Eur. Phys. J. B **82**, 207 (2011).

[48] T. Speck, J. Phys. A: Math. Theor. **44**, 305001 (2011).

[49] A. Ryabov, M. Dierl, P. Chvosta, M. Einax, and P. Maass, J. Phys. A: Math. Theor. **46**, 075002 (2013).

[50] A. single particle system in a thermally isolated box expanding and compressing at a constant speed was considered in R. C. Lua and A. Y. Grosberg, J. Phys. Chem. B **109**, 6805 (2005); I. Bena, C. Van den Broeck, and R. Kawai, Europhys. Lett. **71**, 879 (2005).

[51] A. Gomez-Marin, T. Schmiedl, and U. Seifert, J. Chem. Phys. **129**, 024114 (2008).

[52] R. E. Spinney and I. J. Ford, Phys. Rev. Lett. **108**, 170603 (2012); Phys. Rev. E **85**, 051113 (2012); I. J. Ford and R. E. Spinney, *ibid.* **86**, 021127 (2012).

[53] H. K. Lee, C. Kwon, and H. Park, Phys. Rev. Lett. **110**, 050602 (2013).

[54] C. Kwon, H. Park, J. Yeo, and H. K. Lee (unpublished).

[55] The stationary distribution for general muti-dimensional linear diffusion systems with positive definite D ($\epsilon > 0$) can be found in [27,56,57].

[56] C. W. Gardiner, *Handbook of Stochastic Methods for Physics, Chemistry and the Natural Sciences*, 2nd ed. (Springer, Berlin, 1985).

[57] H. Risken, *The Fokker-Planck Equation*, 2nd ed. (Springer, Berlin, 1989).

[58] G. L. Eyink, J. L. Lebowitz, and H. Spohn, J. Stat. Phys. **83**, 385 (1996).

[59] L. Onsager and S. Machlup, Phys. Rev. **91**, 1505 (1953); S. Machlup and L. Onsager, *ibid.* **91**, 1512 (1953).

[60] A similar property was found also in two-dimensional linear diffusion systems in the overdamped limit [27].